



# Lightworks, a scientific research framework for the design of stiffened composite-panel structures using gradient-based optimization

Sascha Dähne<sup>1</sup> · Edgar Werthen<sup>1</sup> · David Zerbst<sup>1</sup> · Lennart Tönjes<sup>1</sup> · Hendrik Traub<sup>2</sup> · Christian Hühne<sup>1</sup>

Received: 19 June 2023 / Revised: 4 March 2024 / Accepted: 5 March 2024  
© The Author(s) 2024

## Abstract

Efficient structural optimization remains integral in advancing lightweight structures, particularly concerning the mitigation of environmental impact in air transportation systems. Varying levels of detail prove useful for different applications and design phases. The *lightworks* framework presents a modular approach, for the consideration of individual design parameterizations and structural solvers for the numerical optimization of thin-walled structures. The framework provides the combination of lightweight fibre composite design and the incorporation of stiffeners for a gradient-based optimization process. Therefore, an analytical stiffener formulation is implemented in combination with different continuous composite material parameterizations. This approach allows the analysis of local buckling modes, as well as the consideration of load redistribution between stringer and skin. The flexibility achieved in this way allows a tailored configuration of the optimization problem to the required level of complexity. A verification of the framework's implementation is carried out using established literature results of a simplified unstiffened wing box structure, where a very good agreement is shown. The accessibility of solvers with different fidelity through a generic solver interface is demonstrated. Furthermore, the usage of the implemented continuous composite parameterizations as design variables is compared in terms of computational performance and mass, providing different advantages and disadvantages. Finally, introducing stringer into the wing box use case demonstrates a 38% mass reduction, showcasing the potential of the inline optimization of stiffeners.

**Keywords** Lamination parameter · Smearred stiffener · Composite wing · Optimization · Framework · Python

## 1 Introduction

The environmental impact of aviation increases with the rapid growth of air travel and transport. A major contribution to the aircraft fuel burn is driven by the structural elasticity and weight. Deriving efficient structural designs with respect to the overall aircraft is a challenging task and sets different requirements for a design strategy.

Due to their wide range of possible engineering properties and the superior strength-to-weight ratio, laminated

composites have been proven to be very efficient for structural design of lightweight components (Jutte and Stanford 2014). Commercial aircraft with composite wings are already on the market with the Airbus A350 and the Boeing 787. To achieve the minimum possible weight for a composite structure, it is necessary to have an appropriate model that accurately represents its physical properties and takes the optimization strategy into account. In order to handle the increasing complexity of today's aircraft design, the structural system has to be evaluated with respect to the overall efficiency in multidisciplinary design optimization (MDO) workflows (Ghadge et al. 2022; Corrado et al. 2022). Nikbakt et al. (2018) discuss available optimization strategies for composite structures, including non-gradient-based and gradient-based optimization. For MDO applications gradient-based methods have been enforced during the recent past (Martins and Kennedy 2021; Abu-Zurayk et al. 2023). Therefore structural optimization has to provide numerical gradients. The usage of gradients in turn requires a continuous formulation of the design parameters. In addition

---

Responsible Editor: Gang Li

✉ Sascha Dähne  
sascha.daehne@dlr.de

<sup>1</sup> Institute of lightweight Systems, German Aerospace Center, Lilienthalplatz 7, 38108 Braunschweig, Germany

<sup>2</sup> Institute of Mechanics and Adaptronics, Technische Universität Braunschweig, Langer Kamp 6, 38106 Braunschweig, Germany

to a composite parameterization the modelling of stiffeners is an important task to exhaust the structural performance, as discussed in Wunderlich and Dähne (2017); Jutte and Stanford (2014). To the author's knowledge the combination of the adequate representation of composite materials and the design of stiffeners within a gradient-based optimization process is not yet shown comprehensively.

However, some capable gradient-based frameworks have been established, full-filling some of the before-mentioned requirements. The cpacs-MONA framework was designed for the comprehensive aeroelastic design of aircraft (Klimmek et al. 2019; Abu-Zurayk et al. 2020), where a given composite is scaled by thickness. Additionally, a process based on well-established lamination parameter (LP), was demonstrated (Bramsiepe et al. 2018). These represent the complete composite stiffness range by continuous parameters as introduced in Tsai and Pagano (1968). The stiffener elements are pre-sized in cpacs-MONA but they are not resized during the optimization. The structural analysis within cpacs-MONA is based on the commercial Nastran solver. Within the framework presented by Scardaoni and Montemurro (2020) the optimization process is put on a multi-scale FE analysis in ANSYS. Polar parameters are used as design variables, which describe an equivalent plate with continuous parameters, similar to LP. While the approach to handle stiffener is mentioned, the application is not shown and requires explicitly modeled stiffeners. A non-commercial structural analysis is shown with the PROTEUS framework (Werter and De Breuker 2016; Wang et al. 2022) for the conceptual aeroelastic wing design based on beam-models and LP, where stringer are neglected.

However, since the stiffener has a significant influence on the structural elasticity (Wunderlich et al. 2021), the consideration in the optimization process is beneficial. Additionally, the mentioned references provide various strategies on the composite parameterizations, regarding gradient determination, where even more exist (Dykes et al. 2021; Liu et al. 2000). The challenge for the design problem is to provide an accurate physical representation but reduce the amount of design variables and relating design criteria to a minimum, which strongly effect the computational performance.

*lightwoks* now provides a modular framework, in which suitable continuous parameterizations for fibre composites can be combined with a smeared formulation for stringer. This formulation enables the consideration of load redistribution effects during the structural sizing without explicitly modelled stringer. Additionally, this approach allows the design of stringer-stiffened fibre composite skin panels at wing level. Different continuous composite parameterizations are implemented, which can be used to balance the computational cost, correlating with the amount of design variables and the required level of

detail for the optimization. Further flexibility is provided with implemented interfaces for solvers and optimization algorithms. This paper describes the methodology of the structural analysis with an hierarchical panel-meta-model as basis for the optimization and verifies the implementation against results from the literature. The modularity is shown by the application and comparison of three continuous composite parameterizations and two solvers with aligned level of fidelity. Finally the design is enhanced by a stiffened panel concept applied to the same use case.

## 2 Overall process description

To design well performing lightweight structures *lightwoks* uses a gradient-based optimization approach. The objective  $f$  is typically the structural weight for mono-disciplinary optimizations, as presented here.

The general optimization problem, solved by *lightwoks*, can be stated as

$$\begin{aligned} & \underset{\mathbf{x}}{\text{minimize}} && f(\mathbf{x}) \\ & \text{subject to} && x_i^l \leq x_i \leq x_i^u \quad i = 1, \dots, n, \\ & && g_j(\mathbf{x}) \leq 0 \quad j = 1, \dots, m, \end{aligned} \quad (1)$$

where  $\mathbf{x}$  denotes the  $n$  design variables. These variables adjust the objective and can be of different nature, e.g. composite parameter, with individual design ranges and geometric entities like the stiffener height, which is  $> 0$ . The  $m$  constraints  $\mathbf{g}$  have to be considered, which are defined to be  $\leq 0$  and refer to the structural requirements for strength and stability, but also for laminate feasibility boundary conditions.

*lightwoks* is implemented using Python as programming language, which it is widely used in scientific community. An input for the optimization is provided by a CPACS (Common Parametric Aircraft Configuration Schema (Alder et al. 2020)) file. The CPACS schema defines how to parametrically describe air transportation systems in a hierarchical xml structure. It is used as exchange format for multidisciplinary design processes. From such an input file the wing geometry, material distributions and loads are read and used for optimization.

The whole process is generally divided into the optimization and the structural analysis. To give an overview over the optimization process Fig. 1 shows an extended design structure matrix (XDMS (Lambe and Martins 2012)) of the optimization process.

The optimizer, or better the numerical optimization algorithm, drives the optimization iterations. A parameter vector  $\mathbf{x}$  describes the current state and is passed to the optimization processor. The optimization processor is the main interface for a numerical optimization algorithm and takes care of

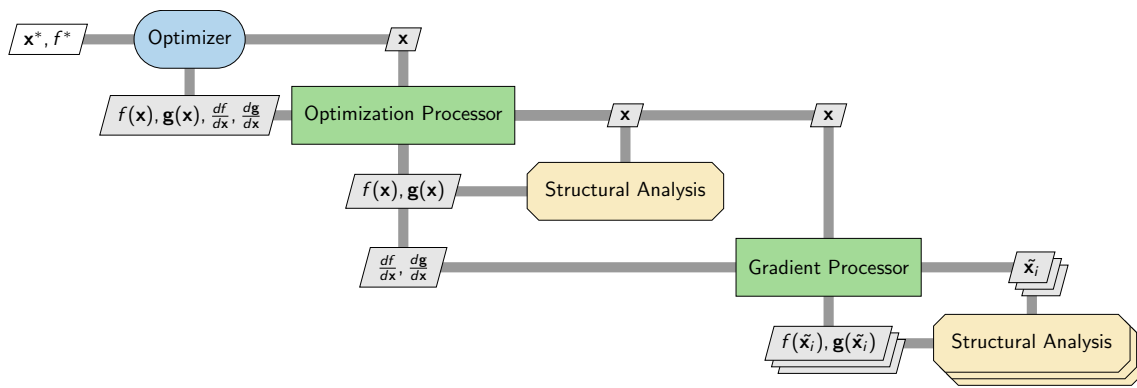


Fig. 1 XDSM Lambe and Martins (2012) representation of *lightworks* architecture with the contributing modules and the optimization data flow

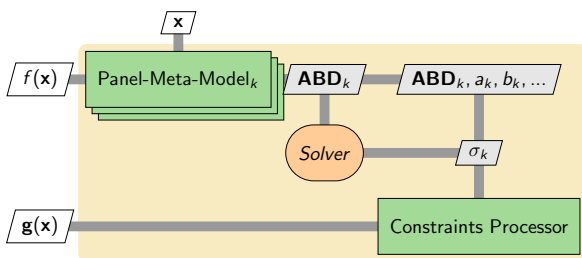


Fig. 2 XDSM Lambe and Martins (2012) representation of *lightworks* structural analysis process

the evaluation of the objective  $f$ , the constraint and their gradients with respect to  $x$ .

At first a structural analysis is performed to determine  $f(x)$  and  $g(x)$ , in parallel the gradient processor determines their sensitivities by finite differences. Multiple varied parameter vectors  $\tilde{x}$  are evaluated by the structural analysis and their responses  $(f(\tilde{x}), g(\tilde{x}))$  are used to approximate their gradients. A detailed description of the structural analysis, which is used multiple times within the optimization, is shown in Fig. 2.

For every  $k$  optimization regions, defined in the CPACS input file, an analytical panel-meta-model is created, where material properties and geometrical dimensions are stored. Independent of the panel being stiffened or not, an **ABD**-Matrix is determined to update the solver model with the current parameters  $x$ . Where the **ABD**-Matrix defines the relation between strain ( $\epsilon$ ) and curvature ( $\kappa$ ) and the force ( $n$ ) and moments ( $m$ ) per unit width, defined in equation 2.

$$\begin{Bmatrix} \{n\} \\ \{m\} \end{Bmatrix} = \begin{bmatrix} [A] & [B] \\ [B] & [D] \end{bmatrix} \begin{Bmatrix} \{\epsilon\} \\ \{\kappa\} \end{Bmatrix} \quad (2)$$

The solver transforms the given external loads into element loads, based on the stiffness provided by the panel-meta-model and the geometry defined by CPACS. With the provided stress field for all optimization regions and all defined

load cases, in combination with the panel stiffness and their geometrical properties, design constraints can be evaluated. A detailed description of the structural analysis, which is a key feature of *lightworks*, is given in the following Sect. 3.

### 3 Structural analysis methods

The core of the *lightworks* optimization process is the structural analysis with an internal panel-based meta-model, where a closer look on the used methods is given in the current section. This analysis is distributed to different modelling levels, with a hierarchical object structure shown in Fig. 3.

Starting from the top level, the solver receives a global **ABD** stiffness for each panel, defined between ribs and spars, and returns an internal load state applied to the panel edges of the *lightworks* internal meta-model. At this panel level global buckling stability is evaluated. On the next lower level the load is redistributed to the stiffened panel elements based on their stiffness, in order to calculate local buckling constraints. The **ABD**-Matrices of the stiffened panel components are provided by different composite parameterizations on the skin level. Those parameterizations represent the design variables and can be chosen. Where the before-mentioned levels describe the structures geometry, the skin only has the thickness dimension. Here, strength and strain limits can be evaluated for the whole laminate. In case that discrete plies should be analyzed, a next lower level can be taken into account to constitute the laminates **ABD**, where strength criteria with respect to the individual plies are considered. In the following sections the implementation is explained in detail.

#### 3.1 Smeared stiffener approach

A discrete modelling of the stiffener in the solver model induce the number of stiffeners as a discrete variable and

**Fig. 3** Hierarchical structure of the *lightworks* internal structural analysis model

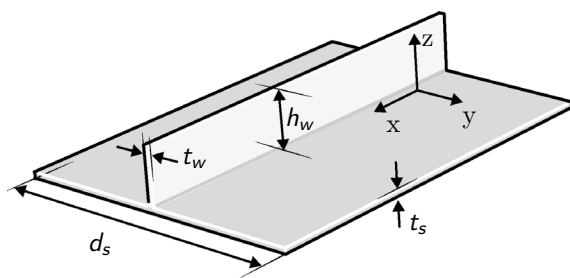
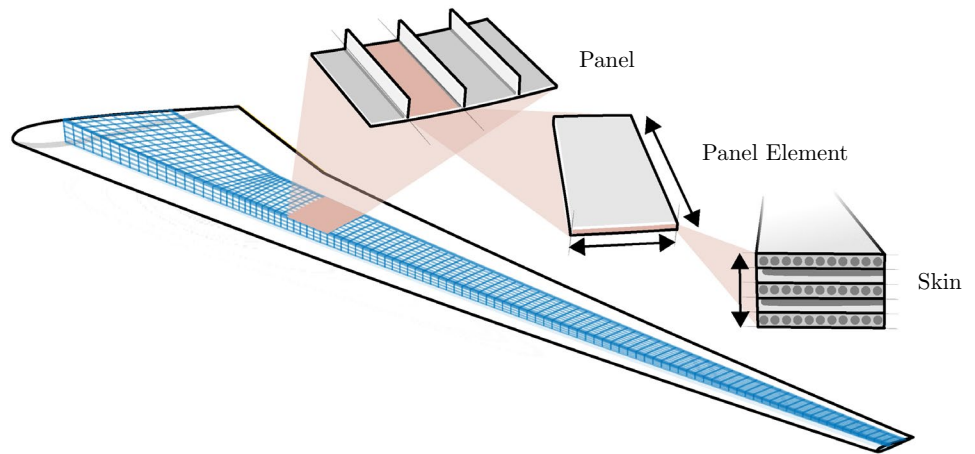


**Fig. 4** Representing stiffened panel element with design variables

increase the model building effort. A variation of a discrete modeled stiffener changes the mesh and induce numerical differences. To overcome this limitation, a smeared approach is used, where the stiffness of the stiffener is calculated analytically and added to the stiffness of the skin cover, while the mesh keeps constant.

The aim of a smeared approach is to simplify the modelling process, to increase the analysis speed and to provide numerical exact gradients due to the analytical formulation.

Nemeth (2011) explained the construction of a smeared stiffener. The basic idea is the formulation of stiffened panel stiffness in terms of **ABD**–Matrices. This approach uses the superposition of skin and stiffener stiffness terms.

Assuming an equal stiffener spacing, the analysis of a panel with multiple stiffeners can be reduced to the analysis of a representing stiffened panel element of the width  $d_s$  as shown in Fig. 4. The  $(x, y, z)$ –axes are the global panel reference axes. The transformation of the stiffener properties into the global coordinate system  $(x, y, z)$  can be done according to the classical laminate theory (CLT) by rotating strains, stress resultants and moment resultants, which represents a rotation of the stiffener around the  $z$  axis. The offset of the stiffness weighted center to the global reference  $x - y$ –plane is denoted with  $\bar{z}_s$ .

The stiffener **ABD**–terms can generally be derived based on averaged  $E$ –modulus  $E_s$ , the cross-sectional area  $A_s$  of the stiffener, the in-plane effective shear correction factor for stiffeners  $k_y^s$ , an effective shear modulus  $G_s$ , the effective moment of inertia  $I_{yy}^s$  and the effective torsional constant for stiffeners  $J_s$ , as follows.

$$\begin{aligned} \bar{\mathbf{A}}^{\text{stiffener}} &= \begin{pmatrix} \frac{E_s A_s}{d_s} & 0 & 0 \\ 0 & 0 & 0 \\ 0 & 0 & \frac{k_y^s G_s A_s}{4d_s} \end{pmatrix} \\ \bar{\mathbf{B}}^{\text{stiffener}} &= \begin{pmatrix} \frac{E_s A_s \bar{z}_s}{d_s} & 0 & 0 \\ 0 & 0 & 0 \\ 0 & 0 & \frac{k_y^s G_s A_s \bar{z}_s}{4d_s} \end{pmatrix} \\ \bar{\mathbf{D}}^{\text{stiffener}} &= \begin{pmatrix} \frac{E_s I_{yy}^s}{d_s} & 0 & 0 \\ 0 & 0 & 0 \\ 0 & 0 & \frac{G_s J_s}{4d_s} \end{pmatrix} \end{aligned} \quad (3)$$

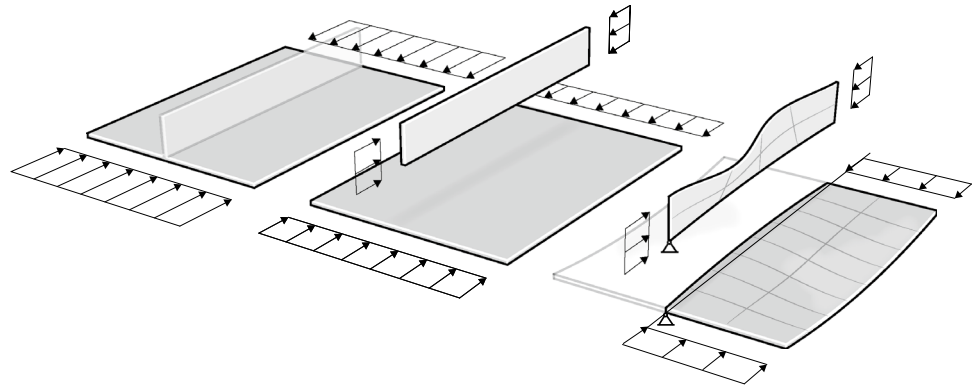
The stiffness of the stiffened plate can be derived by superposing the skin and the stiffener stiffness, related to the same reference plane.

$$\begin{aligned} \mathbf{A}^{\text{panel}} &= \mathbf{A}^{\text{skin}} + \mathbf{A}^{\text{stiffener}} \\ \mathbf{B}^{\text{panel}} &= \mathbf{B}^{\text{skin}} + \mathbf{B}^{\text{stiffener}} \\ \mathbf{D}^{\text{panel}} &= \mathbf{D}^{\text{skin}} + \mathbf{D}^{\text{stiffener}} \end{aligned} \quad (4)$$

Figure 5 explains the steps from a stiffened panel to a base panel. On the stiffened panel shown left in Fig. 5, global buckling can be evaluated. With the information about the element stiffnesses, the load can be distributed over the elements as shown in the middle. Local buckling can then be evaluated on these elements assuming simply supported boundary conditions as a conservative approach.

This approach is verified against finite element models with explicit modeled blade-stiffener by the author for

**Fig. 5** Process of load redistribution and analysis for the analytical smeared stiffened panel



stiffener heights (Dähne and Hühne 2016), for different stiffener rotations (Dähne and Hühne 2018) and for different concepts including the constraint evaluation (Dähne and Werthen 2018) on single panel level without an optimization.

### 3.2 Composite parameterization

The composite design is a special challenge in gradient-based optimization. A composite material is formulated by a stack of rotated base layers, which leads to discrete parameters. Different continuous parameterizations exist for the **ABD**–Stiffness properties of a composite material, with their special advantages and disadvantages. To show the modularity of *lightworks*, three common parameterizations are discussed, which are described hereafter and compared later in Sect. 4.5 for the design optimization.

A straight-forward approach is the definition of a fixed stacking using the individual layer thicknesses as continuous design variables. The **ABD**–Matrix can be written as function of the single ply stiffness  $Q_{ij,k}$  with

$$ABD_{ij} = \sum_{k=1}^N \bar{Q}_{ij,k}(z_k - z_{k-1}). \tag{5}$$

This approach is, among others, used in wind energy applications e.g. in Dykes et al. (2021) and Werthen et al. (2023), where a fixed order of materials is given and only the thicknesses are adjusted. This ensures the desired order of material.

A further approach is the usage of a continuous ply share  $n$  for a common ply angle set of  $0^\circ$ ,  $90^\circ$  and  $\pm 45^\circ$ –plies given in percentage. The formulation of the **ABD** is given with

$$A_{ij} = n_0(\bar{Q}_{ij}) + n_{\pm 45}(\bar{Q}_{ij}) + n_{90}(\bar{Q}_{ij}), \tag{6}$$

$$D_{ij} = \frac{T^2}{12} \cdot A_{ij} \tag{7}$$

and  $B_{ij} = 0$ . This allows a precise description of the in-plane properties with only three variables, while symmetry and balance is ensured. The out-of-plane stiffness **D** is approximated by assuming a homogeneous material distribution over the thickness. The approach is well-suited for structural optimization due to the low amount of design variables and the given laminate feasibility as applied by Liu in Liu et al. (2000). However, the design space of represented composite laminates is only limited, by neglecting the layer order and assume a homogeneous distribution.

A third approach to parameterize composites representing the whole design space, is the usage of the continuous LP. The formulation is based on an equivalent composite plate and was first introduced by Tsai and Pagano (1968). It allows the transformation of the problem into a convex design space. The **ABD**–Matrix is formulated as a linear combination of the material invariants and the LP representing the layer orientation angles to be used as continuous variables in a gradient-based optimization. The matrix entries of the **ABD**–matrix are build up based on the reduced stiffness of each single ply. As example the matrix entry ( $A_{11}$ ) is the sum of the products of ( $\bar{Q}_{11}$ ) and the related ply thickness for every laminae  $k$ . ( $\bar{Q}_{11}$ ) can be split into three parts as derived by Jones (1999). One constant part ( $U_1$ ) which is not affected by the orientation angle ( $\theta$ ) and two frequency components ( $U_2 \cos 2\theta$ ) and ( $U_3 \cos 4\theta$ ) varying with ( $\theta$ ). ( $U_1$ ) to ( $U_5$ ) denote the five material invariants calculated with the single, non-transformed material stiffnesses ( $Q_{ij}$ ) as shown in equation 8.

$$\begin{cases} U_1 = \frac{1}{8}(3Q_{11} + 3Q_{22} + 2Q_{12} + 4Q_{66}) \\ U_2 = \frac{1}{2}(Q_{11} - Q_{22}) \\ U_3 = \frac{1}{8}(Q_{11} + Q_{22} - 2Q_{12} - 4Q_{66}) \\ U_4 = \frac{1}{8}(Q_{11} + Q_{22} + 6Q_{12} - 4Q_{66}) \\ U_5 = \frac{1}{8}(Q_{11} + Q_{22} - 2Q_{12} + 4Q_{66}) \end{cases} \tag{8}$$



$$\begin{aligned}
 A_{11} &= \sum_{k=1}^N \bar{Q}_{11,k}(z_k - z_{k-1}) \\
 &= \sum_{k=1}^N (U_1 + U_2 \cos(2\theta) + U_3 \cos(4\theta))_k (z_k - z_{k-1})
 \end{aligned}
 \tag{9}$$

$$\begin{aligned}
 A_{11} &= U_1 \sum_{k=1}^N (z_k - z_{k-1}) + U_2 \sum_{k=1}^N \cos(2\theta_k)(z_k - z_{k-1}) \\
 &\quad + U_3 \sum_{k=1}^N \cos(4\theta_k)(z_k - z_{k-1}) \\
 &= U_1 T + U_2 V_1 + U_3 V_2
 \end{aligned}
 \tag{10}$$

In total 12 lamination parameters and the total thickness are required to describe the stiffness behavior of a laminated composite. The definition of the stiffness entries as a function of the lamination parameters and the material invariants are given in equation 8. Using 13 parameters allow to describe the complete stiffness properties of arbitrary laminates whether they are symmetric, balanced or non of this. All terms are precisely described including the out-of-plane stiffness, which is most relevant for stability. Assuming symmetric and balanced laminates and restricting to 0°, 90° and ± 45°-plies, the number of parameters can be reduced to 6 for the complete design space.

$$\begin{aligned}
 &\begin{Bmatrix} A_{11}, B_{11}, D_{11} \\ A_{22}, B_{22}, D_{22} \\ A_{12}, B_{12}, D_{12} \\ A_{66}, B_{66}, D_{66} \\ A_{16}, B_{16}, D_{16} \\ A_{26}, B_{26}, D_{26} \end{Bmatrix} = \left[ T, \frac{T^2}{4}, \frac{T^3}{12} \right] \\
 &\cdot \begin{bmatrix} 1 & V_1^{*A,B,D} & V_2^{*A,B,D} & 0 & 0 \\ 1 & -V_1^{*A,B,D} & V_2^{*A,B,D} & 0 & 0 \\ 0 & 0 & -V_2^{*A,B,D} & 1 & 0 \\ 0 & 0 & -V_2^{*A,B,D} & 0 & 1 \\ 0 & V_3^{*A,B,D}/2 & V_4^{*A,B,D} & 0 & 0 \\ 0 & V_3^{*A,B,D}/2 & -V_4^{*A,B,D} & 0 & 0 \end{bmatrix} \begin{Bmatrix} U_1 \\ U_2 \\ U_3 \\ U_4 \\ U_5 \end{Bmatrix}
 \end{aligned}$$

### 3.3 Constraints

A structural optimization is constraint by design criteria and often by feasibility restrictions. The following section describes the special feasibility constraint for lamination parameter and the typical structural design criteria.

The convexity of the lp design space was first shown by Grenestedt and Gudmundson (1993) and is also the assumption for the usage of LP within the *lightworks* framework. In literature, there are several numerical and analytical approaches proposed to create a feasible domain

for different combinations of ply angles. The investigated concepts are limited to a certain dimension, usually 4- or 5D. The analytical formulation of Diaconu et al. (2002) is limited to symmetric and balanced laminates with a ply angle set of 0°, 90° and ±45°-plies which reduced the number of LP to five. Also the numerical or mixed approaches are not proven for higher dimensions then 5D (Macquart et al. (2018) and Werthen and Dähne (2018)) due to the computational limitations when creating point meshes or clouds. The complexity grows exponentially with the dimension  $\propto n_{points}^{O(dimension)}$ .

Up to now there is no mathematical formulation available to describe the complete 12D-space of LP as a constraint. The *lightworks* framework uses the reduced set of five LP for symmetric and balanced laminates and ply angles of 0°, 90° and ±45°. The constraint formulation is based on hyperplanes given in Werthen and Dähne (2018), which are linear and therefore easy differentiable. The design space forms a convex hull by hyperplanes in the 5D space. Additional constraints to ensure producible layups can be formulated with respect to ply continuity (Seresta et al. 2007) or blended laminates (Liu et al. 2011) in longitudinal direction between two adjacent panels. Both is considered with the 5D LP space according to Werthen and Dähne (2018).

The intact structure is ensured by physical limits to avoid critical failure modes. Commonly failure criteria of composites are evaluated with the help of the layer-wise stress level, caused by the outer loading of the structure.

A criterion for laminate strength was formulated for the LP design space by Khani et al. (2011) which is used in here. It formulates the strength criterion in the LP space by using a conservative failure envelope for all ply angles. Also a rotation of the main stiffness axis for composites is taken into account. The strength envelope can be determined solving equation 11.

$$C_{ij}\epsilon_i\epsilon_j + rC_i + r^2c_0 = 0, \quad i, j = I, II \tag{11}$$

Another common approach is the usage of strain limits as a criterion to ensure intact laminae, without knowing the discrete stacking sequence (Liu et al. 2011, 2000; Seresta et al. 2007). The used criterion is shown in equation 12.

$$g_{strength} = \max \left\{ \frac{\epsilon_x}{F_x}, \frac{\epsilon_y}{F_y}, \frac{\epsilon_{xy}}{F_{xy}} \right\} - 1 \tag{12}$$

Bending and torsion of an aircraft wing causes compression and tension loads in the wing covers and shear loads in the spars as sizing load states. Therefore the evaluation of structural stability is indispensable. The critical buckling load is formulated on the basis of the **ABD**-Matrix and the geometrical dimensions of an orthotropic plate given in HSB

45111-08 (Working group Structural Analysis (IASB) 2009) for compression loads shown in equation 13 and in HSB 45112-02 (Working group Structural Analysis (IASB) 2009) shown in equation 14 for shear loads.

$$\begin{aligned}
 n_{x,cr} &= k_x(\bar{\alpha}, \beta) \cdot \frac{\pi^2}{b^2} \sqrt{D_{11}D_{22}} \\
 \bar{\alpha} &= \frac{a}{b} \cdot \sqrt[4]{\frac{D_{22}}{D_{11}}} \\
 \beta &= \frac{D_{12} + 2D_{33}}{\sqrt{D_{11}D_{22}}}
 \end{aligned}
 \tag{13}$$

$$n_{s,cr} = k_s(\beta) \cdot \left(\frac{\pi}{b}\right)^2 \sqrt[4]{D_{11}D_{22}^3} \tag{14}$$

Where a and b are the length and width of the plate and  $k_x$  is the buckling coefficient for compression buckling and  $k_s$  for shear, respectively. For a bend-twist coupled wing a combined load state of compression and shear loading occurs which require the usage of a combined safety factor calculated by equation 15, where  $R = n_{allowed}/n_{current}$

$$R_x + R_s^2 \leq 1 \tag{15}$$

As already described with Fig. 5, the equation 15 can be applied to the whole panel for global buckling and to the individual elements for local stability evaluation.

All constraints are formulated in the form  $g_j \leq 0$ , where  $g_j$  are the individual constraint values.

### 4 Verification and analysis of the flexible composite design optimization strategy

Within the following section the proposed optimization strategy of the *lightworks* framework is applied to a wing box design problem from literature. On that use case the implementation is verified and some results on the computational scalability are presented. In order to demonstrate and to assess the advantages of the frameworks flexibility, a comparison of two designs derived from two solvers providing different fidelity levels. Further, a comparison of the implemented continuous composite parameterizations is carried out. Additionally, an optimization is shown taking the stiffener influence into account, with the introduced stiffened panel approach.

#### 4.1 Least weight problem definition

In order to verify the presented approach a use case is chosen, that is used in previous works to analyse different issues on composite optimization (Scardaoni and Montemurro 2020; Panettieri et al. 2019; Liu et al. 2011; Seresta et al. 2007; Liu et al. 2000). There, a simple rectangular wing box represents the structural model as target of

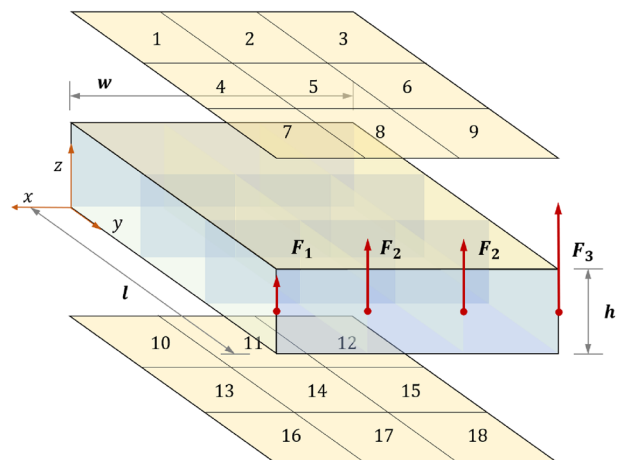


Fig. 6 Wing box example use case, with:  $l = 3543$  mm;  $w = 2240$  mm;  $h = 381$  mm;  $F_1 = 90009.77$  N;  $F_2 = 187888.44$  N;  $F_3 = 380176.16$  N and the panel numeration

the optimization, illustrated in Fig. 6. The wing box is clamped at the root section and loaded with four asymmetric transverse forces on the wing tip. Both the lower and upper cover comprise nine design regions for the optimization bounded by four equally spaced spars and ribs, that are fixed to a shear layup of  $[(\pm 45^\circ)_{22}]$ . The numeration of a total of 18 panels is shown in Fig. 6

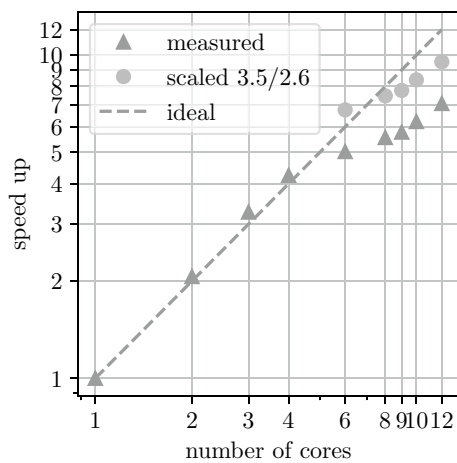
The composite materials that are used in literature are listed in Table 1, where the used material of Scardaoni and Montemurro (2020) differ from the other references. Both materials are considered for verification in Sect. 4.3 as used in the references.

As input for the design optimization studies a model is created into the CPACS format, as described in Sect. 2. All CPACS files are available from the public repository in Dähne and Zerbst.

As described in Sect. 2, within *lightworks* an external solver converts external loads to internal loads and solves the displacement field. The obtained load states are provided to the panel-meta-model for the internal evaluation. The solver, that is used to obtain the results below, is the finite element solver B2000++ [36]. The requirements for interacting with *lightworks* are fulfilled by providing shell elements in combination with specific ABD-Properties. The linear static solver used in the present work, provides fast displacements and element loads. A model for the use case described below is created, with the help of a CPACS interface, which is used to access geometry and material objects from the CPACS input file. The open source tool Gmsh (Geuzaine and Remacle 2009) is used to automatically create the finite element mesh. The finite element model has 558 quadrilateral shell elements. 15 elements are evenly distributed over the wing box length, 9 over width

**Table 1** Material properties used for rectangular wing box case according to literature

Property	Unit	Mat.1	Mat.2
		Panettieri et al. (2019); Liu et al. (2011); Seresta et al. (2007); Liu et al. (2000)	Scardaoni and Montemurro (2020)
$E_{xx}$	(GPa)	127.56	181
$E_{yy} = E_{zz}$	(GPa)	13.03	10.3
$\nu_{xy} = \nu_{xz}$	(-)	0.3	0.27
$\nu_{yz}$	(-)	-	0.42
$G_{xy} = G_{xz}$	(GPa)	6.41	7.17
$G_{yz}$	(GPa)	4.5	3.78
$\rho$	(kg m <sup>-3</sup> )	1577.76	1760
$X_{T/C}$	( $\epsilon$ /MPa)	0.008 (0.08 Liu et al. (2011))	1500
$Y_{T/C}$	( $\epsilon$ /MPa)	0.029	246
$S$	( $\epsilon$ /MPa)	0.015	68

**Fig. 7** Parallel scalability for the gradient determination process

and 3 over height. The root is clamped and the forces are connected via multi-point-constraint elements.

For the numerical optimization the publicly available interface package pyOptSparse (Wu et al. 2020) is used to make the optimizer SNOPT 7.7 (Gill et al. 2018) available.

## 4.2 Parallel scalability study

The most computationally expensive step for the optimization process is the determination of gradients. Accordingly, this process is distributed to parallel cores. In order to analyse the *lightworks* performance, a study was carried out, investigating how the calculation time scales with the number of cores on the basis of the presented least weight problem (4.1).

All calculations are performed on a Intel(R) Xeon(R) CPU E5-2690 v3 @ 2.60GHz with 12 physical cores. All 12 cores are used in parallel to evaluate the gradients. The

gradient determination scales very well with the number of cores as shown in Fig. 7.

The analysis shows that the problem scales ideal up to four cores with a maximum frequency of 3.5GHz. Afterwards the cpu has the lower nominal rating of 2.6GHz. Scaling the values starting from six cores with the turbo boost ratio brings the speed up ratio back to nearly ideal. Thus, the *lightworks* framework constitutes a good basis for large problems, e.g. in MDO, where a high computational efficiency is required.

## 4.3 Verification of the *lightworks* process based on literature results

In order to verify the presented approach and the implementation, literature results are taken as reference cases to compare with. Three references are used as verification cases, where different approaches, tools and parameterizations are used. The three references are hereinafter referred as Ref.1 up to Ref.3 to simplify the identification.

Ref.1 is chosen from Seresta et al. (2007), where discrete laminate stackings are optimized with a genetic algorithm. Liu et al. (2011), chosen as Ref.2, proposed a two level approach. A gradient-based optimization with LP is used at the first level and in the second level discrete stackings are retrieved. A small deviation is done here for Mat.1, where a higher allowable for max strain in  $x$ -direction is referred in the literature. The results from the first level are used for comparison. Scardaoni and Montemurro (2020) finally applied a gradient-based optimization using polar parameter to parameterize the composite material, which is the Ref.3. All the references use commercial FE-Solvers and utilize manufacturing criteria such as blending constraints. The differences in the used references are summarized in Table 2.



**Table 2** Summary of the differences in the used literature references

	lightworks	Ref.1 Seresta et al. Seresta et al. (2007)	Ref.2 Liu et al. Liu et al. (2000)	Ref.3 Scardaoni et al. Scardaoni and Montemurro (2020)
Solver	B2000++	GENESIS	ANSYS	ANSYS
Optimization Type	Gradient Based	GA	Gradient Based	Gradient Based
Parameterization	LP	Discrete Stacking	LP	Polar Parameter
Stability Method	Analytical	Analytical	Numerical	Numerical
Strength Method	Max Strain/Strength	Max Strain	Max Strain	Strength
Material	Mat.1/Mat.2	Mat.1	Mat.1	Mat.2

maximum frequency of For the verification analysis the use case is optimized with *lightworks* using equivalent material properties and strength methods.

Despite of Ref.2 all panels are optimized individually. Ref.2 couples the three panels in *x*-direction to reduce the number of variables, which is done in the present approach as well. The optimization problem has 108 parameter for Ref.1 and Ref.3 and 36 for Ref.2. Feasibility constraints, one stability for each panel and one strength constraint for each element in a design region are present. Further constraints arise from the manufacturing constraints for LP described in Sect. 3.3 summing up to 1490 and 902 for Ref.2.

The results in terms of the panel-wise thickness distribution is shown in Fig. 8 for all three verification cases. The panels 1-9 constitute the upper cover. Due to the bending-torsional loading it is driven subject to shear buckling stability, which results in a higher thickness in all cases. The

panels 10-18 are the lower cover and are plotted below the thicknesses of the upper cover. The sizing criterion is the tensile strength due to the upward bending. In comparison with Ref.1 Fig. 8a shows a very good agreement with the presented approach. At the tip a slight difference arise, where the load is applied. Ref.1 obtained a total mass for the cover panels of 232.9kg, while the presented approach results in 226.2kg. Detailed results are given in Table 3.

The laminate stiffness is shown as polar plot regarding the in-plane stiffness in Fig. 9. On the upper cover  $\pm 45^\circ$  ply orientations are dominant, which respects the stability driven design. On the lower cover  $0^\circ$  ratios are higher, which reflects the tensile strength dominated design.

The coupling of the three panels in *x*-direction following Ref.2 reveals a close thickness distribution as well. The coupled design regions have the same parameters and properties, but stability and strength is evaluated individually. Especially

**Table 3** Optimization results for Ref.1 configuration

Panel	$t_s$ [mm]	$V1_{A,s}$	$V2_{A,s}$	$V1_{D,s}$	$V2_{D,s}$	$V3_{D,s}$	$g_{max}$	Critical
1	14.43	-0.29	-0.44	-0.03	-0.95	0.00	5e-6	buck
2	18.66	-0.07	-0.44	0.01	-0.95	0.01	1e-6	buck
3	22.3	0.12	-0.38	0.00	-0.94	-0.00	3e-5	buck
4	12.39	-0.23	-0.56	-0.02	-0.97	-0.00	1e-6	buck
5	15.85	-0.01	-0.56	-0.00	-0.97	0.00	6e-7	buck
6	18.63	0.11	-0.33	-0.00	-0.93	-0.00	7e-6	buck
7	9.21	-0.34	-0.33	-0.04	-0.93	-0.01	3e-5	buck
8	10.57	-0.23	-0.56	-0.02	-0.97	-0.00	-4e-7	buck
9	12.8	-0.01	-0.55	-0.02	-0.97	0.00	7e-5	buck
10	1.43	0.64	0.80	0.20	0.70	-0.04	4e-7	strain
11	3.77	0.85	0.82	0.64	0.57	0.00	-6e-3	strain
12	5.66	1.00	0.95	1.00	0.96	-0.01	4e-7	strain
13	1.05	0.42	0.80	-0.28	0.71	-0.01	-1e-2	strain
14	2.07	0.63	0.82	0.05	0.58	0.04	8e-8	strain
15	3.83	0.85	0.81	0.62	0.56	-0.02	8e-7	buck
16	2.76	0.22	0.81	-0.54	0.75	0.04	-8e-7	buck
17	3.19	0.42	0.84	-0.24	0.67	-0.06	-1e-6	buck
18	4.0	0.63	0.81	0.05	0.56	0.05	-8e-7	buck

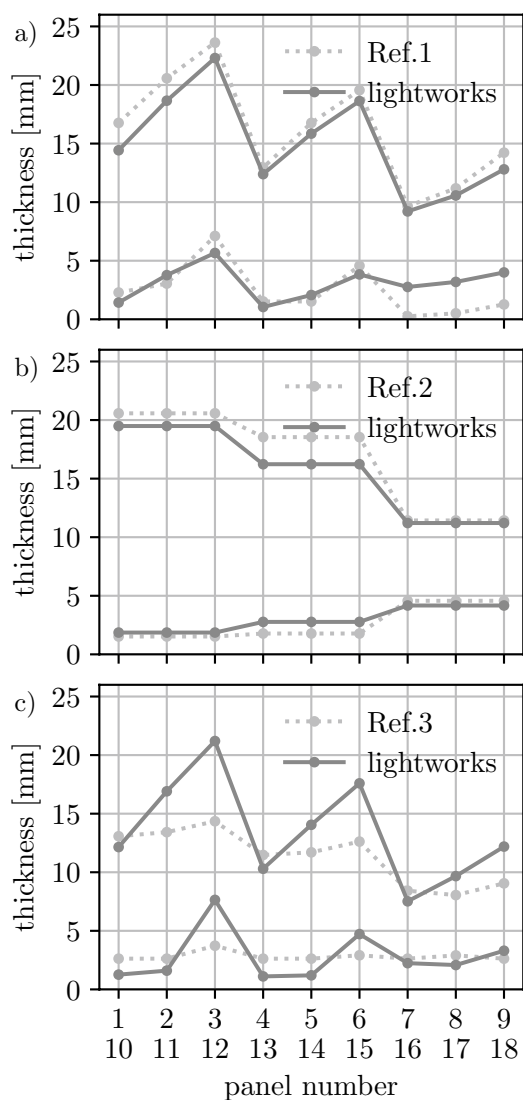


**Fig. 8** Thickness comparison of *lightworks* with reference results according to Table 2 a Ref.1, b Ref.2, c Ref.3

in the middle section a stiffness redistribution between upper and lower cover can be observed in Fig. 8b. The total mass of Ref.2 is 237.93kg. The *lightworks* mass of 232.7kg is very close, although Ref.2 is using numerical stability analysis instead of the more conservative analytical approach used in *lightworks* based on simple supported boundary condition at the edges.

Ref.3 use a less conservative buckling criterion, which leads to lower thicknesses on the upper cover. Additionally, a different strength criterion is applied with respect to the polar parameter representation. Ensuring the same basis for the comparison, the strength criterion for LP based on Khani et al. (2011) is considered. The strength dominated lower cover is in contrast to the upper cover in accordance with the presented results (Fig. 8c). A mass delta of ~14% can be observed by comparing the total cover panel masses. The

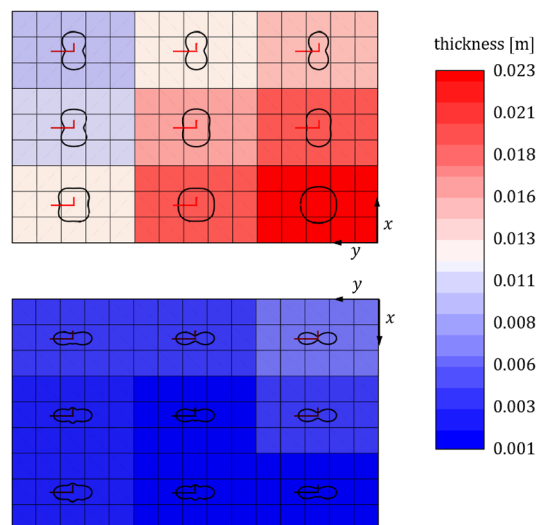


**Fig. 9** *lightworks* polar plot results and thickness distribution referring to Ref.1

detailed results for Ref.2 and Ref.3 are shown in Table 6 and Table 7, respectively.

#### 4.4 Comparison of designs based on solver models with different fidelity

In order to demonstrate the capabilities of a flexible solver interface, two structural solvers with different fidelity levels are compared within a design optimization. Both solvers are inhouse tools with full access to the code and without any limitations in the number of parallel executions, due to licence restrictions. This allows a parallel determination of gradients by using finite differences.

The first solver is the finite element solver B2000++, where the used model is already described in Sect. 4.1.

The second one is a beam-based solver named PreDoCS, providing high computational efficiency. Here, the wing structure is described as a longitudinal beam, where stresses are calculated analytically on span-wise discrete cross-sections (Werthen et al. 2023). The used beam theory is based on the approach of Jung et al. (2002), which includes, beside the basic bending and extension, the shear and torsional degrees of freedom, which is essential for wing-like structures.

The panel-meta-model is identical for both solvers and therefore the criteria and the parameterization too. LP and skin thicknesses are used as design variables for the unstiffened model, as already described in Sect. 4.3.

Figure 10 shows the resulting thickness distributions. Especially the thickness on the upper cover of the PreDoCS design is smoother, which is an effect of the beam model and the cross-sectional load distribution. The

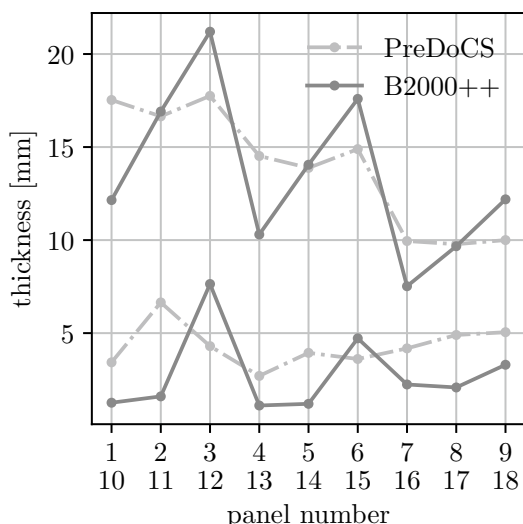


Fig. 10 Thickness results of two solvers with different levels of fidelity within the *lightworks* design process

finite element model shows higher differences in thickness between adjacent panels as a result of load peaks at the edges, especially at the higher loaded rear edge.

The difference in total cover panel mass is 252.6kg for the PreDoCS solver, which is conservative compared to 227.7kg using the B2000++ finite element solver. This means a delta of ~11%. However, the resulting masses and the thickness distributions are in a good agreement.

Where the time to solve the structural problem takes 1.01s for B2000++, it is 0.42s. Due to the fact, that the gradient calculation is the most expensive part of the computation (see Sect. 4.2), the solving step does not effect the overall optimization time that much, in case of such simple model. Nevertheless, this effect scales with the size of the model, which is much larger for typical wing design use cases, and also with the number of designing load cases.

### 4.5 Comparison of designs from different composite parameterizations

To demonstrate the flexibility of the design problem in terms of composite models, three different continuous parameterizations are implemented (Sect. 3.2) and compared to each other. The study is performed according to Table 2 with the maximum strain criterion and Mat.1 except of the parameterization. The convergence behavior is shown in Fig. 11. An equivalent stopping criterion is used for all three optimizations. The change of the objective have to be smaller than  $1 \times 10^{-3}$  and the sum of failing constraints have to be less than  $1 \times 10^{-4}$  as shown in equation 16.

Table 4 Parameterization performance indicators

	Individual Layer Thickness	Ply Share	Lamination Parameter
num. parameters	72	54	108
num. constraints	2218	328	1210
num. Iterations	63	44	79
mass [kg]	227.07	223.68	218.18

$$\Delta f \leq 1 \times 10^{-3} \sum g_i \leq 1 \times 10^{-4} \text{ if } g_i \geq 0. \tag{16}$$

In Table 4 an overview of the amount of design variables is given, together with the number of iterations until a converged solution is obtained. It can be seen that the consumed iterations correlate with the size of the optimization problem, in terms of parameter and constraints.

The ply share approach needs only three variables for each panel, which is the thickness and two of three ratios of  $0^\circ, 45^\circ, 90^\circ$ . Therefore, it provides the fastest convergence with 44 iterations. The resulting mass is 223.68kg. For the individual layer thickness a stacking of  $[45, 90, -45, 0]_s$  is used, where the individual layer thicknesses are the design variables. Due to their order, which might not be optimal, the highest mass of 227.07kg is achieved. Of course, this result depends on the predefined stacking, and thus can be improved with the input. However, a refined input stacking would also increase the number of variables. The number of constraints is much higher than the other approaches, due to the layer-wise strength evaluation. The LP provided the lowest mass with 218.18kg, due to it's comprehensive design space. The prize to pay is reflected in the highest number of iterations to converge (Fig. 11).

### 4.6 Results of stiffened panel design optimization

Using the panel-meta-model allows adding stiffener without changing the solver model. A stiffener with an initial height of 100mm and a constant spacing of  $d_s$  of 200mm is defined as starting point for the optimization. The stiffener are oriented inwards.

The layup of the web is set to  $[0, 45, 90, -45, 0]_s$  and the corresponding LP are kept fix for the stiffeners, for sake of simplicity. Only the thickness of the web is an additional design variable as well as the web height. Hence, the stiffened design adds two design variables per panel and two additional constraints for the optimization, being web buckling and local buckling stability. The increased problem size extends the convergence from the computational perspective (Fig. 12). On the other hand, the structural benefit of stiffeners, to increase critical buckling stresses on

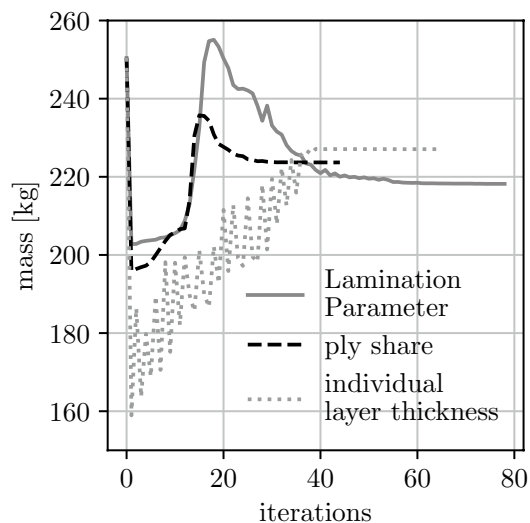


**Fig. 11** Mass and convergence behavior of the least weight design with implemented composite parameterizations

the upper cover, are obvious and the mass saving potential is in the order of 38% for this use case, where the mass is reduced from 218.18kg to 135.2kg. The detailed results are given in the appendix in Table 5.

The dominant design criterion that sizes the structure is changes with adding stiffeners from global buckling to local skin buckling between the stiffeners on the upper shell. On the lower shell global panel buckling come into play due to reduced skin thicknesses.

## 5 Conclusion

This paper introduces an optimization process for composite structures assembled from thin shells incorporating unstiffened and stiffened designs. The framework

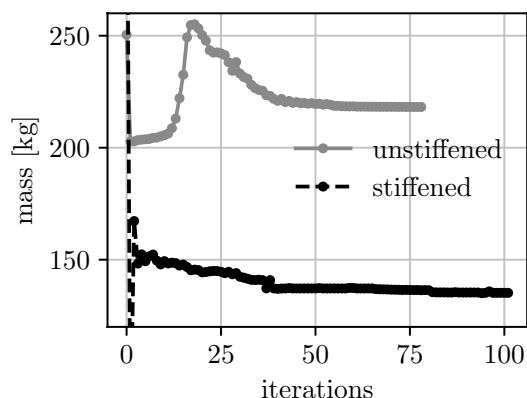


**Fig. 12** Mass and convergence behavior of the least weight design including and excluding the stiffener

implementations are presented describing the modular structured approach to combine structural analysis and numerical optimization. Changes on the structural analysis can be separated from the optimization, by an internal panel meta-model.

A Verification of the presented approach is performed based on three literature results using a common academic use case. While the accordance of the results is very high for most of the references, not all results could be met, due to methodical differences. Nevertheless, the implementation is accurate within the methodical boundaries.

Three composite parameterizations are implemented to an internal panel meta-model and compared in terms of final objective and convergence to show the benefits of the configurable design approach. While an increasing accuracy yield a better objective and a preferable composite design, the number of parameters and constraints and, in consequence, the number of iterations increases too.

Furthermore, a smeared stiffener approach is implemented and extended with different composite parameterizations. The applicability of this approach is applied to the common use case and a mass reduction of 38% could be demonstrated.

The connection of solvers with different level of fidelity is demonstrated by comparing a finite element solver with a beam-based solver, while identical criteria and material properties are used. The results show methodical driven effects, like the consideration of peak loads at edges with finite elements and differences in the load and thickness distribution between both solver. However, a good agreement is shown in the optimized stiffnesses, where the beam solver provides superior calculation efficiency.

The flexibility in the configuration of the design problem provides a broad usability of the proposed framework for lightweight engineering. The approach can be used to support the aircraft design from the conceptual design phase with fast methods, combining low-fidelity solvers and composite models, up to high-fidelity finite element models and composite parameterizations, capturing the whole laminate design space.

The computational cost to determine gradients is the main driver in the evaluation time. Therefore more time efficient gradient determination concepts should be emphasised. In addition, more precise gradient information could improve the convergence and reduce the number of iterations.

A common problem coming along with the continuous parametrization of laminates is the derivation of discrete plies, based on an optimized thickness and stiffness distribution. The layup retrieval will be focussed in further research to analyse the manufacturability of obtained wing designs.

### Appendix A optimization results

**Author contributions** Conceptualization: Sascha Dähne David Zerbst and Hendrik Traub; Methodology: Sascha Dähne, Edgar Werthen, Lennart Tönjes; Formal analysis and investigation: Sascha Dähne, David Zerbst, Edgar Werthen; Writing - original draft preparation: Sascha Dähne, David Zerbst, Edgar Werthen, Lennart Tönjes; Writing - review

See Tables 5, 6, 7

**Table 5** Results for stiffened configuration

Panel	$t_s$ [mm]	$V1_{A,s}$	$V2_{A,s}$	$V1_{D,s}$	$V2_{D,s}$	$V3_{D,s}$	$t_w$ [mm]	$V1_{A,w}$	$V2_{A,w}$	$V1_{D,w}$	$V2_{D,w}$	$V3_{D,w}$	$d_s$ [mm]	$h$ [mm]
1	6.47	0.38	-0.29	0.04	-0.91	-0.01	7.69	0.20	0.20	0.34	0.30	0.24	200.00	60.27
2	7.62	0.50	-0.07	0.12	-0.80	0.02	9.04	0.20	0.20	0.34	0.30	0.24	200.00	66.36
3	8.99	0.61	0.17	0.21	-0.60	0.01	10.80	0.20	0.20	0.34	0.30	0.24	200.00	72.59
4	5.21	0.27	-0.53	0.02	-0.97	0.00	6.21	0.20	0.20	0.34	0.30	0.24	200.00	52.64
5	6.54	0.38	-0.29	0.04	-0.91	-0.00	7.92	0.20	0.20	0.34	0.30	0.24	200.00	60.30
6	7.47	0.50	-0.07	0.12	-0.80	-0.00	8.96	0.20	0.20	0.34	0.30	0.24	200.00	65.30
7	3.76	0.05	-0.51	-0.02	-0.96	-0.02	4.18	0.20	0.20	0.34	0.30	0.24	200.00	43.99
8	4.50	0.17	-0.29	-0.01	-0.91	-0.00	4.92	0.20	0.20	0.34	0.30	0.24	200.00	49.40
9	5.19	0.37	-0.23	0.03	-0.88	0.01	5.61	0.20	0.20	0.34	0.30	0.24	200.00	54.18
10	1.65	1.00	0.95	0.97	0.89	0.01	0.10	0.20	0.20	0.34	0.30	0.24	200.00	23.87
11	3.52	1.00	0.95	0.97	0.90	0.01	0.10	0.20	0.20	0.34	0.30	0.24	200.00	24.61
12	5.38	1.00	0.95	0.97	0.90	0.00	0.10	0.20	0.20	0.34	0.30	0.24	200.00	20.00
13	1.09	0.82	0.86	0.51	0.61	0.00	0.10	0.20	0.20	0.34	0.30	0.24	200.00	37.92
14	2.01	0.90	0.82	0.70	0.52	0.00	0.10	0.20	0.20	0.34	0.30	0.24	200.00	36.19
15	3.31	0.88	0.74	0.64	0.33	0.02	0.10	0.20	0.20	0.34	0.30	0.24	200.00	20.00
16	1.23	0.61	0.85	-0.00	0.66	0.04	0.10	0.20	0.20	0.34	0.30	0.24	200.00	64.20
17	1.65	0.70	0.86	0.18	0.61	0.00	0.10	0.20	0.20	0.34	0.30	0.24	200.00	80.90
18	1.77	0.73	0.75	0.28	0.35	-0.01	0.10	0.20	0.20	0.34	0.30	0.24	200.00	85.55

**Table 6** Results for Ref.2

Panel	$t_s$ [mm]	$V1_{A,s}$	$V2_{A,s}$	$V1_{D,s}$	$V2_{D,s}$	$V3_{D,s}$
1	19.49	-0.21	-0.60	-0.01	-0.98	0.02
2	19.49	-0.21	-0.60	-0.01	-0.98	0.02
3	19.49	-0.21	-0.60	-0.01	-0.98	0.02
4	16.23	-0.32	-0.37	-0.03	-0.94	-0.00
5	16.23	-0.32	-0.37	-0.03	-0.94	-0.00
6	16.23	-0.32	-0.37	-0.03	-0.94	-0.00
7	11.21	-0.34	-0.33	-0.04	-0.93	0.01
8	11.21	-0.34	-0.33	-0.04	-0.93	0.01
9	11.21	-0.34	-0.33	-0.04	-0.93	0.01
10	1.86	0.06	0.44	-0.41	0.21	0.31
11	1.86	0.06	0.44	-0.41	0.21	0.31
12	1.86	0.06	0.44	-0.41	0.21	0.31
13	2.77	0.02	0.40	-0.41	0.13	0.34
14	2.77	0.02	0.40	-0.41	0.13	0.34
15	2.77	0.02	0.40	-0.41	0.13	0.34
16	4.17	0.12	0.65	-0.49	0.40	0.19
17	4.17	0.12	0.65	-0.49	0.40	0.19
18	4.17	0.12	0.65	-0.49	0.40	0.19



**Table 7** Results for Ref.3

Panel	$t_s$ [mm]	$V1_{A,s}$	$V2_{A,s}$	$V1_{D,s}$	$V2_{D,s}$	$V3_{D,s}$
1	12.53	-0.34	-0.33	-0.04	-0.93	0.01
2	16.60	-0.12	-0.33	0.00	-0.93	-0.00
3	20.57	0.10	-0.33	0.00	-0.93	-0.01
4	10.56	-0.34	-0.33	-0.04	-0.93	-0.01
5	14.17	-0.12	-0.33	-0.00	-0.93	-0.00
6	17.24	0.10	-0.33	-0.00	-0.93	-0.00
7	5.60	-0.18	-0.44	-0.03	-0.95	-0.01
8	9.82	0.04	-0.44	-0.03	-0.95	-0.02
9	11.80	0.26	-0.45	0.01	-0.95	0.01
10	1.49	0.61	0.57	0.33	0.57	-0.08
11	0.97	0.76	0.71	0.61	0.39	0.00
12	6.80	0.93	0.82	0.78	0.52	-0.00
13	1.49	0.43	0.67	-0.26	0.53	0.03
14	0.93	0.64	0.70	0.10	0.35	-0.09
15	5.06	0.81	0.60	0.60	0.22	-0.16
16	2.07	0.24	0.72	-0.44	0.52	-0.09
17	2.12	0.43	0.67	-0.26	0.53	-0.02
18	3.34	0.59	0.60	0.05	0.22	-0.13

and editing: Christian Hühne, David Zerbst, Hendrik Traub; Software: Sascha Dähne, Lennart Tönjes, Edgar Werthen; Funding acquisition: Christian Hühne; All authors read and approved the final manuscript.

**Funding** Open Access funding enabled and organized by Projekt DEAL. We would like to acknowledge the funding by the Deutsche Forschungsgemeinschaft (DFG, German Research Foundation) under Germany's Excellence Strategy - EXC 2163/1 - Sustainable and Energy Efficient Aviation - Project-ID 390881007 and Germany's Collaborative Research Center - CRC 1463/1 - Integrated design and operation methodology for offshore megastructures - Project-ID 434502799.

**Data availability** All CPACS data-sets generated during the current study are available in the zenodo repository[35].

## Declarations

**Conflict of interest** (include appropriate disclosures) The authors have no competing interests to declare that are relevant to the content of this article.

**Replication of results** All results can be replicated using the CPACS files in the zenodo repository Dähne and Zerbst (2023) and *light-works* version 0.6.0+g45e5beb. Additionally PreDoCS version [0.13+69e8d4fe] and B2000++ version 4.4.3 are used.

**Open Access** This article is licensed under a Creative Commons Attribution 4.0 International License, which permits use, sharing, adaptation, distribution and reproduction in any medium or format, as long as you give appropriate credit to the original author(s) and the source, provide a link to the Creative Commons licence, and indicate if changes were made. The images or other third party material in this article are included in the article's Creative Commons licence, unless indicated otherwise in a credit line to the material. If material is not included in the article's Creative Commons licence and your intended use is not permitted by statutory regulation or exceeds the permitted use, you will

need to obtain permission directly from the copyright holder. To view a copy of this licence, visit <http://creativecommons.org/licenses/by/4.0/>.

## References

- Abu-Zurayk M, Schulze M (2023) Exploring the benefit of engaging the coupled aero-elastic adjoint approach in MDO for different wing structure flexibilities. In: AIAA AVIATION, Forum. AIAA AVIATION Forum, American Institute of Aeronautics and Astronautics, p. 2023
- Abu-Zurayk M, Merle A, Ilic C, Keye S, Goertz S, Schulze M, Klimmek T, Kaiser C, Quero D, Häßy J, Becker R, Fröhler B, Hartmann J, (2020) Sensitivity-based multifidelity multidisciplinary optimization of a powered aircraft subject to a comprehensive set of loads. In: AIAA AVIATION, FORUM, AIAA AVIATION Forum. American Institute of Aeronautics and Astronautics 06:2020
- Alder M, Moerland E, Jepsen J, Nagel B (2020) Recent advances in establishing a common language for aircraft design with CPACS
- Bramsiepe KR Handojo V, Meddaikar YM, Schulze M, Klimmek T (2018) Loads and Structural Optimization Process for Composite Long Range Transport Aircraft Configuration. In: 2018 Multidisciplinary Analysis and Optimization Conference, Atlanta, Georgia American Institute of Aeronautics and Astronautics
- Corrado G, Ntourmas G, Sferza M, Traiforos N, Arteiro A, Brown L, Chronopoulos D, Daoud F, Glock F, Ninic J, Ozcan E, Reinoso J, Schuhmacher G, Turner T (2022) Recent progress, challenges and outlook for multidisciplinary structural optimization of aircraft and aerial vehicles. Prog Aerospace Sci 135:100861
- Dähne S, Hühne C (2016) Efficient gradient based optimization approach of composite stiffened panels in multidisciplinary environment. In: 5th Aircraft Structural Design Conference 2016
- Dähne S, Hühne C (2018) Gradient based structural optimization of a stringer stiffened composite wing box with variable stringer orientation. Conference Name: WCSMO ISBN: 978-3-319-67987-7

- Dähne S, Werthen E (2018) Stringer-concept evaluations with multidisciplinary gradient based optimization of composite wing structures
- Dähne S, Zerbst D (2023) CPACS for Rectangular Box Wing. <https://doi.org/10.5281/zenodo.7972946>
- Diaconu CG, Sato M, Sekine H (2002) Layup optimization of symmetrically laminated thick plates for fundamental frequencies using lamination parameters. *Struct Multidisc Optim* 24(4):302–311
- Dykes Katherine, Andrew Ning S, Scott George, Peter Graf (2021) Wisdem (wind-plant integrated system design and engineering model)
- Geuzaine C, Remacle JF (2009) Gmsh: A 3-D finite element mesh generator with built-in pre- and post-processing facilities. *Int J Num Methods Eng* 79(11):1309–1331
- Ghadge R, Rr Ghorpade, Joshi S (2022) Multi-disciplinary design optimization of composite structures: a review. *Composite Struct* 280:114875
- Gill PE, Murray W, Saunders MA Elizabeth Wong (2018) SNOPT 7.7 User's Manual. Technical report, University of California, San Diego
- Grenestedt P, Gudmundson JL (1993) Layup optimization of composite material structures. *Optimization Design Advanced Material*. Elsevier Science, Amsterdam, pp 311–336
- Jones RM (1999) *Mechanics of composite materials*. Taylor and Francis, New York
- Jung SN, Nagaraj VT, Chopra I (2002) Refined structural model for thin- and thick-walled composite rotor blades. *AIAA J* 40(1):105–116
- Jutte C, Stanford KB (2014) Aeroelastic tailoring of transport aircraft wings: state-of-the-art and potential enabling technologies. Technical Report NASA/TM-2014-218252, L-20395, NF1676L-18677, NASA Langley Research Center, Hampton, VA, United States
- Khani A, Ijsselmuiden ST, Abdalla MM, Gürdal Z (2011) Design of variable stiffness panels for maximum strength using lamination parameters. *Composites Part B: Eng* 42(3):546–552
- Klimmek T, Schulze M, Abu-Zurayk M, Ilic C, Merle A (2019) CPACS-MONA - An independent and in high-fidelity based mdo tasks integrated process for the structural and aeroelastic design of aircraft configurations. In: *International Forum on Aeroelasticity and Structural Dynamics (IFASD 2019)*, page 21, Savannah, Georgia, USA, . Curran Associates, Inc
- Lambe AB, Martins JRRR (2012) Extensions to the design structure matrix for the description of multidisciplinary design, analysis, and optimization processes. *Struct Multidisc Optim* 46(2):273–284
- Liu B, Haftka RT, Akgün MA (2000) Two-level composite wing structural optimization using response surfaces. *Struct Multidisc Optim* 20(2):87–96
- Liu D, Toropov VV, Querin OM, Barton DC (2011) Bilevel optimization of blended composite wing panels. *J Aircraft* 48(1):107–118
- Macquart T, Maes V, Marco Bordogna T, Pirrera A, Weaver PM (2018) Optimisation of composite structures - enforcing the feasibility of lamination parameter constraints with computationally-efficient maps. *Composite Struct* 192:605–615
- Martins JRRR, Kennedy GJ (2021) Enabling large-scale multidisciplinary design optimization through adjoint sensitivity analysis. *Struct Multidisc Optim*. <https://doi.org/10.1007/s00158-021-03067-y>
- Nemeth MP (2011) A treatise on equivalent-plate stiffnesses for stiffened laminated-composite plates and plate-like lattices
- Nikbakt S, Kamarian S, Shakeri M (2018) A review on optimization of composite structures part i: laminated composites. *Composite Struct* 195:158–185
- Panettieri E, Montemurro M, Catapano A (2019) Blending constraints for composite laminates in polar parameters space. *Composites Part B: Eng* 168:448–457
- Scardaoni MP, Montemurro M (2020) A general global-local modeling framework for the deterministic optimisation of composite structures. *Struct Multidisc Optim* 62(4):1927–1949
- Seresta Oh, Gürdal Z, Adams DB, Watson LT (2007) Optimal design of composite wing structures with blended laminates. *Composites Part B: Eng* 38(4):469–480
- SMR SA. B2000++. <https://www.smr.ch/products/b2000/>
- Tsai SW, Pagano NJ (1968) *Invariant properties of composite materials*. Technomic Publishing Company, Lancaster
- Wang Zhijun, Peeters Daniël, De Breuker Roeland (2022) An aeroelastic optimisation framework for manufacturable variable stiffness composite wings including critical gust loads. *Struct Multidisc Optim* 65(10):290
- Werter NPM, De Breuker R (2016) A novel dynamic aeroelastic framework for aeroelastic tailoring and structural optimisation. *Composite Struct* 158:369–386
- Werthen E, Ribnitzky D, Zerbst D, Kühn M, Hühne C (2023) Aerostructural coupled optimization of a rotor blade for an upscaled 25 mw reference wind turbine. *J Phys* 2626(1):012012
- Werthen E, Hardt D, Balzani C, Hühne C (2023) Comparison of different cross-sectional approaches for the structural design and optimization of composite wind turbine blades based on beam models. *Wind Energy Sci* 1–26:2023
- Werthen E, Dähne S (2018) Design- and manufacturing constraints within the gradient based optimization of a composite aircraft wingbox. In *6th Airframe Structural Design Conference*, Working group Structural Analysis (IASB). Aeronautical Engineering Handbook (LTH): Handbook for structural analysis (HSB)
- Wu N, Kenway G, Mader CA, Jasa J, Martins JRRR (2020) Pyopt-sparse: a python framework for large-scale constrained non-linear optimization of sparse systems. *J Open Source Software* 5(54):2564
- Wunderlich T, Dähne S (2017) Aeroelastic tailoring of an NLF forward swept wing. *CEAS Aeronaut J* 8(3):461–479
- Wunderlich TF, Dähne S, Reimer L, Schuster A (2021) Global aerostructural design optimization of more flexible wings for commercial aircraft. *J Aircraft* 58(6):1254–1271. <https://doi.org/10.2514/1.C036301>

**Publisher's Note** Springer Nature remains neutral with regard to jurisdictional claims in published maps and institutional affiliations.